ELSEVIER

Ceramics International 28 (2002) 299–302

CERAMICS
INTERNATIONAL

www.elsevier.com/locate/ceramint

Preparation and characterization of hydroxyapatite suspensions for solid freeform fabrication

Jiemo Tian, Yong Zhang*, Xinmin Guo, Limin Dong

Beijing Fine Ceramics Laboratory, State Key Laboratory of New Ceramics and Fine Processing, Institute of Nuclear Energy Technology, Tsinghua University, PO Box 1021, Beijing 102201, People's Republic of China

Received 8 January 2001; received in revised form 27 April 2001; accepted 15 September 2001

Abstract

A comparative investigation on particle size, zeta potential and rheology behavior of suspensions of hydroxyapatite (HA) powders produced by a wet-chemical synthesis method is presented. Results have shown that temperature and soaking time of the calcination process significantly affects the HA particle size, and results in a reduction of the zeta potential and suspension viscosity. On the basis of the present experimental and calculated results, the reduction in the viscosity is attributed to a higher repulsion barrier in interparticle potential. © 2002 Elsevier Science Ltd and Techna S.r.l. All rights reserved.

Keywords: A. Suspensions; Hydroxyapatite; Zeta potential

1. Introduction

The attractive biocompatibility and bioaffinity of hydroxyapatite (HA) ceramics have led to the widespread use of these materials in clinical applications [1]. In recent years, the drive toward optimal conditions for osteoconduction has created a strong interest in the fabrication technology of HA ceramics. Previously reported processing methods for forming porous HA implants include reticulation technique [2], the near-net-shape process by the metal oxidation route [3] and the use of natural materials such as coral and bone [4]. However, a disadvantage of these methods is the inability to control the structural configuration that affects the biological response. Another disadvantage is that the compressive strength of the ceramic has been found to fall drastically with the increase in pore size and amount of porosity.

Solid Freeform Fabrication (SFF) techniques allow moldless manufacturing of ceramics. The literature describes many SFF or rapid prototyping methods to make complex structures, including stereolithography (SLA) [5], fused deposition modeling (FDM) [6], selective laser sintering (SLS) [7], laminated object manufacturing (LOM) [8], 3D printing [9], etc. Of these, one method based on drop-on demand printing [10] has drawn attention because it shares the knowledge from colloidal processing with the SFF techniques. During this gelation process, a well-dispersed suspension, with high solids loading of reasonably low viscosity to facilitate the doctor blade processing, is required. Hence, rheology of the suspension needs to be studied and modeled, with a focus on the effect of particle size.

In this paper, the influence of the history of processing on zeta potential of HA powders and rheology behavior of HA slurries, was investigated. Further calculation based on the Derjaguin–Landau–Verway–Overbeek (DLVO) theory was carried out to determine the effects of particle size and surface potential on the aqueous suspension.

2. Experimental procedures

2.1. Materials

HA powders were prepared via a wet-chemical synthesis technique, based on the precipitation of HA precursors from aqueous solutions. Triammonium phosphate trihydrate and calcium nitrate tetrahydrate

---

* Corresponding author. Tel.: +86-10-62770238-419; fax: +86-10-69771464.

E-mail address: zhangyong_zh@163.net (Y. Zhang).

0272-8842/02/$22.00 © 2002 Elsevier Science Ltd and Techna S.r.l. All rights reserved.
PII: S0272-8842(01)00094-3

were used as starting chemicals. Ammonium hydroxide was used to adjust the pH value of the mixed solution. The reaction temperature was held at 85 °C. The coprecipitation powder was rinsed with deionized water, filtered, dried, and then calcined at 700 °C for 3 h. The HA powder thus prepared was denoted as HA1. A second HA powder investigated here was HA2, which was produced by the same procedure as HA1, and followed by heat-treating again at 900 °C for 24 h.

2.2. Characterization

XRD analysis was performed using a Rigaku D/max-RB type X-ray diffractometer with CuK$_\alpha$ radiation. The range of scans was $10° \leqslant 2\theta \leqslant 60°$ for the crystalline phase identification, $25.6° \leqslant 2\theta \leqslant 26.3°$ for crystallite size measurement. The scan step was 0.02° with a step time of 2 s. The crystallite size was determined using the Scherrer formula:

$$D = \frac{0.9\lambda}{B\cos\theta} \tag{1}$$

where D is the diameter of the crystal particle, λ the wave length of the X-ray, θ the scattering angle, and B is the broadening of the diffraction line measured at half its maximum intensity.

The zeta potential of the HA powder was measured as a function of pH, using a commercial Brookhaven Zetaplus meter. The pH of the suspension was controlled by using 0.01 N HCl solution as an acid and 0.01 N NaOH as a base and measured with a pH meter (Model 420 Orion Research Inc.).

For each viscosity measurement, standard suspensions of 15 vol.% HA powder in deionized water were prepared. The viscosity of the suspensions was measured on a stress-controlled viscometer (Physica MCR300, Germany) at shear rate from 0.1 to 250 s^{-1}. All viscosity measurements were performed at 25 °C.

3. Results and discussion

The XRD patterns collected from the two powders are shown in Fig. 1. Both samples are highly crystalline. The peaks agree very well with the hexagonal hydroxyapatite structure. For HA2 particles, however, a minimal amount of minor component was observed. X-ray analysis also revealed that the particle size of the two samples, HA1 and HA2, were 65 and 115.1 nm, respectively. The HA2 particles have a significantly larger particle size compared to the HA1 particles. These particle size values are qualitatively consistent with the equivalent spherical particle diameters calculated by using the surface area, which was measured by the Brunauer–Emmett–Teller (BET) method.

The electrophoretic mobility of the two powders was studied as a function of pH. The results are shown in Fig. 2, the zeta potential of HA2 was generally found smaller than that of HA1. A different dispersion behavior can be thus expected for HA2 powders. The viscosity of suspensions of the two powders was measured as a function of the shear rate. As shown in Fig. 3, the viscosity of suspensions of HA1 is higher than that of suspensions of HA2.

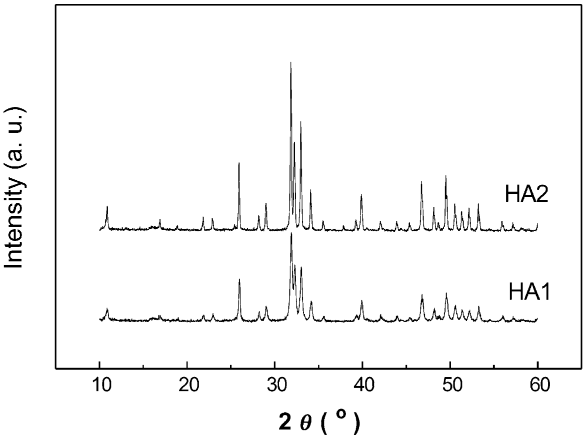

Fig. 1. XRD patterns of HA1 and HA2.

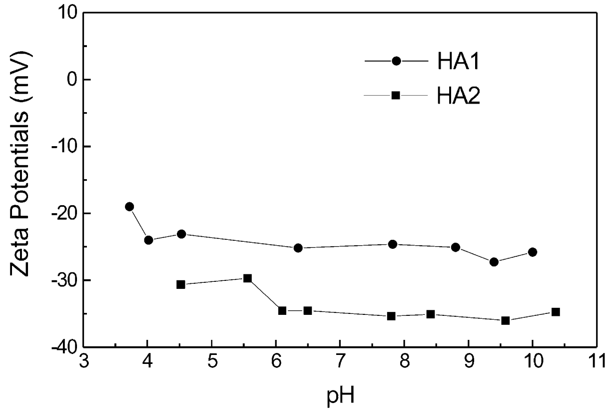

Fig. 2. Zeta-potential vs pH for HA1 and HA2.

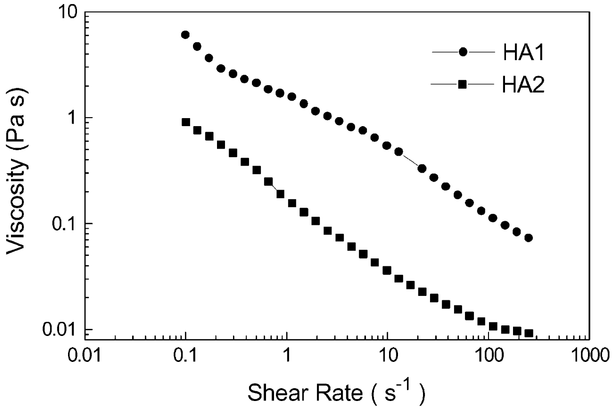

Fig. 3. Viscosity as a function of shear rate for HA1 and HA2.

The zeta potential of HA2 particles at various pH values is around −35 mV, which is obviously smaller than the value of about −25 mV for the HA1 particles. However, the isoelectric point (IEP) for the HA particles was not observed over the range of pH values evaluated. This result may suggest HA particles that have been prepared via precipitation, to be covered by a thin film of specifically adsorbed ions. Additionally, not only the state of material surface but also the history of the material processing strongly influences the zeta potential. The severe calcining process altered the surface potential of the HA particles, as evidenced by the viscosity measurements. As can be seen from Fig. 3, the viscosity of suspensions of HA2 displays a lower state over a wide range of shear rates.

To probe the difference between the rhelogical behavior of suspensions, the interaction potential between two spherical particles at surface separation distance D was calculated according to the well-known DLVO theory. By combining the attractive van der Waals interaction free energy $V_{\mathrm{vdW}}(D)$, and the repulsive double layer repulsion $V_{\mathrm{DL}}(D)$, the overall net interaction energy $V(D)$ is given by [11]:

$$V(D) = V_{\mathrm{vdW}}(D) + V_{DL}(D) \tag{2}$$

providing that the interaction distance is much smaller than the particle size R, that is, $D < < R$, V(D) can be approximated by [12,13]:

$$V(D) = 2\pi\varepsilon_0\varepsilon R\varphi^2\exp(-\kappa D) - \frac{AR}{12D} \tag{3}$$

where R is the particle radius, ε_{o} the permittivity of a vacuum, ε the dielectric constant of water (78.5), φ the surface potential of the particles, A the Hamaker constant. κ is the Debye–Huckel reciprocal length parameter and is written by:

$$\kappa = \left(\frac{1000e^2N_A}{\varepsilon_o\varepsilon k_B T}\sum Z_i^2 M_i\right)^{1/2} \tag{4}$$

where e is electronic charge, N_{A} the Avogadro's number, k_B the Boltzmann constant, T the temperature, Z_i and M_i are the charge and the molar concentration of species i in the solution.

The particle radius of HA1 and HA2 are 32.5 and 57.55 nm, respectively. Considering that it is difficult to measure the surface potential exactly, the surface potentials of HA1 and HA2 are assumed approximately equal to the zeta potentials shown in Fig. 2. The zeta potentials used in the interaction-energy calculations for HA1 and HA2 at pH = 7 are −25 mV and −35 mV, respectively. For the HA particle the Hamaker constant in water is unavailable now due to lack of necessary optical data on HA [14]. Here, we assume the Hamaker constant of HA to be 6×10^{-20} J, in view of the reported Hamaker constant of inorganic materials with the same crystal structure [15]. Meanwhile, the Debye parameter κ is taken as 1.04×10^6 m^{-1}, which derived from the Eq. (4) using the corresponding electrolyte concentration.

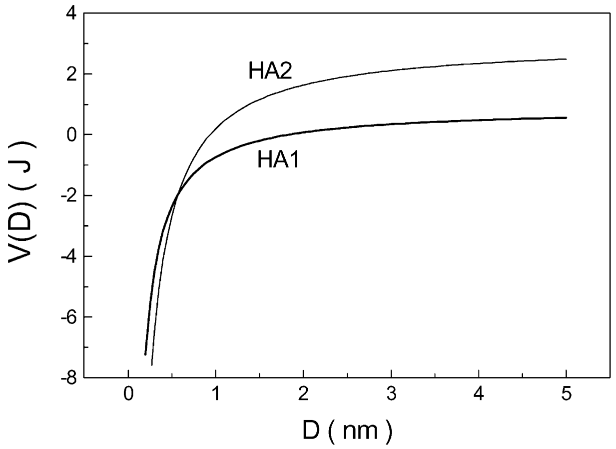

Fig. 4. The calculated DLVO interparticle interaction potential of HA1 and HA2 powders.

The calculated DLVO potentials for HA1 and HA2 are shown in Fig. 4. It is noted that the barrier height for HA2 powders is higher than for HA1 powders. As a result, the suspension viscosity decreases with the increase of the repulsion barrier. The higher barrier in the interaction energy of HA2 powder is due to the larger particle size and the smaller zeta potential in comparison with HA1 powder.

4. Conclusions

Submicrometer-sized, single-phase hydroxyapatite bioceramic powders, denoted as HA1, have been synthesized via a chemical precipitation technique. Another HA powder HA2 was obtained by calcining the HA1 at 900 °C for 24 h. XRD measurements revealed that the second heat treatment at a higher temperature for a longer time produced a larger size. Compared to HA1 powders, the HA2 powders show a smaller zeta potential value over the range of pH values investigated, indicating that the severe calcining process altered the surface potential of the HA particles. The rheological properties of aqueous suspensions of the HA1 and HA2 powders are reported. In rheological tests, it was found that the second calcination reduces the viscosity of the suspensions over a wide range of shear rates. The DLVO potential calculation showed that the barrier height in the interaction energy between HA2 particles is higher than that for HA1 particles, thus leading to the reduction in the viscosity.

Acknowledgements

The work was supported by National Key Foundation Project (973) under Contract No. G19990647-02.

References

[1] L.L. Hench, Bioceramics, a clinical success, Am. Ceram. Soc. Bull. 77 (7) (1998) 67–74.

[2] B.S. Chang, C.K. Lee, K.S. Hong, H.J. Youn, H.S. Ryu, S.S. Chung, K.W. Park, Osteoconduction at porous hydroxyapatite with various pore configurations, Biomaterials 21 (2000) 1291–1298.

[3] E. Saw, K.H. Sandhage, P.K. Gallagher, Near-net-shaped calcium hydroxyapatite by the oxidation of machinable, calcium-bearing precursors (the volume identical metal oxidation, or VIMOX, process), J. Am. Ceram. Soc. 83 (2000) 998–1000.

[4] S. Joschek, B. Nies, R. Krotz, A. Gopferich, Chemical and physicochemical characterization of porous hydroxyapatite ceramics made of natural bone, Biomaterials 21 (2000) 1645–1658.

[5] C. Hull. Apparatus for production of three-dimensional objects by stereolithography, US Patent 4575330, 1986.

[6] M.K. Agarwala, A. Bandyopadhyay, R.V. Weeren, A. Safari, S.C. Danforth, N.A. Langrana, V.R. Jamalabad, P.J. Whalen, FDC, rapid fabrication structural components, Am. Ceram. Soc. Bull. 75 (11) (1996) 60–65.

[7] F. Klocke, H. Wirtz, Selective laser sintering of ceramics, laser-assisted net-shape engineering 2, in: Proceedings of the LANE'97, 1997, pp. 589–596.

[8] C.W. Griffin, J. Dautenbach, S. Mcmillin, Desktop manufacturing: LOM vs pressing, Am. Ceram. Soc. Bull. 73 (8) (1994) 109–113.

[9] E. Sachs, M. Cima, P. Williams, D. Brancazio, J. Cornie, Three dimensional printing: rapid tooling and prototypes directly from a CAD model, J. Eng. Ind 114 (1992) 481–488.

[10] S. Baskaran, G.D. Maupin, G.L. Graff, Freeform fabrication of ceramics, Am. Ceram. Soc. Bull. 77 (7) (1998) 53–58.

[11] W.M. Sigmund, N.S. Bell, L. Bergstrom, Novel powder-processing methods for advanced ceramics, J. Am. Ceram. Soc. 83 (2000) 1557–1574.

[12] W.H. Shih, D. Kisailus, W.Y. Shih, Y.H. Hu, J. Hughes, Rheology and consolidation of colloidal alumina-coated silicon nitride suspensions, J. Am. Ceram. Soc. 79 (1996) 1155–1162.

[13] J.A. Lewis, Colloidal processing of ceramics, J. Am. Ceram. Soc. 83 (2000) 2341–2359.

[14] L. Bergstrom, private communication.

[15] L. Bergstrom, Hamaker constants of inorganic materials, Adv. Colloid Interface Sci. 70 (1997) 125–169.